

# Coexistence of two dune growth mechanisms in a landscape-scale experiment

Ping Lü<sup>1</sup>, Clément Narteau<sup>2</sup>, Zhibao Dong<sup>1</sup>, Philippe Claudin<sup>3</sup>, Sébastien Rodriguez<sup>2</sup>, Zhishan An<sup>4</sup>, Cyril Gadal<sup>2</sup>, Sylvain Courrech du Pont<sup>5</sup>

<sup>1</sup> School of Geography and Tourism, Shaanxi Normal University, Xi'an, China.

<sup>2</sup> Université de Paris, Institut de physique du globe de Paris, CNRS, Paris, France.

<sup>3</sup> Physique et Mécanique des Milieux Hétérogènes, CNRS, ESPCI PSL Research Univ, Sorbonne Univ, Université de Paris, Paris, France.

<sup>4</sup> Northwest Institute of Eco-Environment and Resources, Lanzhou, China.

<sup>5</sup> Laboratoire Matière et Système Complexes, CNRS, Université de Paris, Paris, France.

An edited version of this paper was published by AGU. Copyright 2020 American Geophysical Union: Lü, P., Narteau, C., Dong, Z., Claudin, P., Rodriguez, S., An, Z., Gadal, C. & Courrech du Pont, S. (2022). Coexistence of two dune growth mechanisms in a landscape-scale experiment. *Geophysical Research Letters*, e2021GL097636. <https://doi.org/10.1029/2021GL097636>.

## Key Points:

- Dunes of different shapes and orientations develop and coexist under the same natural wind regime depending on sand availability.
- The dynamics of pattern coarsening selects dune aspect-ratio over short time.
- There is a minimum size for dune elongation on a nonerrodible bed, below which barchan or asymmetric barchan shapes are observed.

---

Corresponding author: Clément Narteau, [narteau@ipgp.fr](mailto:narteau@ipgp.fr)

**Abstract**

In landscape-scale experiments at the edge of the Gobi desert, we show that various dune types develop simultaneously under natural wind conditions. Using 4 years of high-resolution topographic data, we demonstrate that, depending on sand availability, the same wind regime can lead to two different dune orientations, which reflect two independent dune growth mechanisms. As periodic oblique dunes emerge from a sand bed and develop to 2 meters in height, we analyze defect dynamics that drive the non-linear phase of pattern coarsening. Starting from conical sand heaps deposited on gravels, we observe the transition from dome to barchan and asymmetric barchan shapes. We identify a minimum size for arm elongation and evaluate the contribution of wind reversals to its longitudinal alignment. These experimental field observations support existing theoretical models of dune dynamics boosting confidence in their applicability for quantitative predictions of dune evolution under various wind regimes and bed conditions.

**Plain Language Summary**

Dune fields are characterized by the occurrence of both isolated dunes and periodic bedforms of variable shape and orientations. However, there is no field evidence whether these isolated and periodic dune patterns develop at the same time and from the same growth mechanism. Here, by leveling neighboring parcels of a dune field, we perform landscape-scale experiments with controlled initial and boundary conditions to test the influence of sand availability on the formation and timescales associated with the development of both types of patterns. Starting from a flat sand bed, we observe the emergence of periodic dunes and measure for more than 3 years how they grow as they interact with each other. Over the same time period, by regularly feeding sand heaps deposited nearby on a non-erodible bed, we observe how dune shape changes, eventually leading to the elongation of isolated dunes with a different orientation. These experiments are unique by their size and duration. Under natural conditions, they show that the same wind regime can be associated with two dune growth mechanisms depending on sand availability. The coexistence of these two dune growth mechanisms provides a basis for examining the diversity of dune shapes on Earth or other planetary bodies depending on local environmental conditions.

## 1 Introduction

Dunes record information about the environmental flows in which they formed and represent powerful (paleo-)environmental proxies on Earth and other planetary bodies (Ewing et al., 2010; Fenton & Hayward, 2010; Lorenz & Zimbelman, 2014; Lapôtre et al., 2016, 2021; Chanteloube et al., 2022). However, given the variety of boundary and initial conditions to be considered, a major question has been to assess the relative contribution of current and past wind regimes to the diversity of dune size, shape and orientation (Kocurek & Ewing, 2005; Ewing & Kocurek, 2010; Parteli et al., 2009; Telfer et al., 2018; Lapôtre et al., 2018). To conduct this inverse problem, there is still a lack of reliable experiments on eolian dune growth under natural wind regimes. Notably, the elongation of isolated dunes on a nonerrodible bed has never been experimentally validated in the field and compared to the dynamics of periodic dune patterns in areas of abundant sediment supply - a prerequisite to better understand the coexistence of dunes with different orientations and the impact of seasonal wind reversals on eolian landscapes within sand seas.

Sand availability recognized early as an important factor in dune morphodynamics (Bagnold, 1941; Wasson & Hyde, 1983), but its strong influence on dune growth mechanism has only recently been formalized by Courrech du Pont et al. (2014). Past research mainly focused on the dune instability that arises over an unlimited layer of loose sand (Kennedy, 1963; Richards, 1980; Andreotti et al., 2002; Gadal et al., 2019; Gadal, Narteau, Ewing, et al., 2020; Delorme et al., 2020). Over short timescales, the linear regime of this instability is responsible for the emergence of periodic dunes, assuming that all modes (wavelengths) grow exponentially independently from each other (Lü et al., 2021). Over longer timescales, a non-linear regime of dune pattern coarsening dominated by collisions and interactions between bedforms leads to an increase in dune amplitude and wavelength in space and time (Gao, Narteau, & Rozier, 2015; Gadal, Narteau, Ewing, et al., 2020; Jarvis et al., 2022). In areas of limited sediment supply, dunes adopt crescentic shapes that can also elongate by depositing at their tips the sediment that is transported along their crests (Parteli et al., 2009; Reffet et al., 2010; Zhang et al., 2012; Courrech du Pont et al., 2014; Lucas et al., 2014; Gao, Narteau, Rozier, & Courrech du Pont, 2015; Lucas et al., 2015; Lü et al., 2017; Fernandez-Cascales et al., 2018; Gadal, Narteau, Courrech du Pont, et al., 2020). These two dune growth mechanisms rely differently on sand fluxes perpendicular to the crest. According to dune-instability theory for unlimited sed-

iment supplies, bedforms align along the direction for which the sum of crest-normal fluxes reaches a maximum, i.e., the direction of highest growth rate (Rubin & Hunter, 1987; Ping et al., 2014; Gadal et al., 2019). Alternatively, dunes may elongate in the direction that allows crest-normal fluxes from both sides of the crest to cancel each other out. This is the reason why elongation requires at least bidirectional wind regimes and why, under specific multidirectional regimes, star-dune arms can grow in various directions (Zhang et al., 2012).

Using a set of landscape-scale experiments, we investigate here the formation and development of dunes in different conditions of sand availability to assess the coexistence of these two dune growth mechanisms. Collected data are analyzed to test under natural wind conditions the predictions of Courrech du Pont et al. (2014) regarding dune shape, orientations and dynamics (growth, migration or elongation), as well as the associated sand fluxes at their crests. In addition, these data are used to quantify the relationships between defect density, wavelength and amplitude of periodic dune patterns during the coarsening phase in areas of unlimited sediment supply, and the characteristic length-scales associated with the elongation phase of dunes lying on a non-erodible bed (Rozier et al., 2019).

## **Landscape-Scale Experiments**

Field experiments were continuously conducted from October 2013 to November 2017 in the Tengger Desert at the southeastern edge of the Gobi basin in China, an area exposed to a bimodal wind regime (Ping et al., 2014). Two main experiments have been performed. The elongating dune experiment started in October 2013 by placing two conical sand heaps 2.5 and 3 m high on a flat gravel bed isolated from the incoming sand by straw checkerboards (Fig. 1a). To the southwest, pre-existing dunes were also leveled in April 2014 to form a flat rectangular bed 100 m long and 75 m wide (Figs. 1b,c). The main axis of this sand bed experiment was aligned with the direction of the primary wind, which blows from the northwest mainly in the spring when the Siberian high-pressure system weakens (Fig. 1d). In summer, the easterly wind of the east-Asian monsoon dominates. This bimodal wind regime has a divergence angle of  $146^\circ$  and a transport ratio of 1.5, so that all conditions to observe both growth mechanisms are met according to theory and numerical simulations (Courrech du Pont et al., 2014; Gao, Narteau, Rozier, & Courrech du Pont, 2015). Sand heaps are located far enough from the sand bed ex-

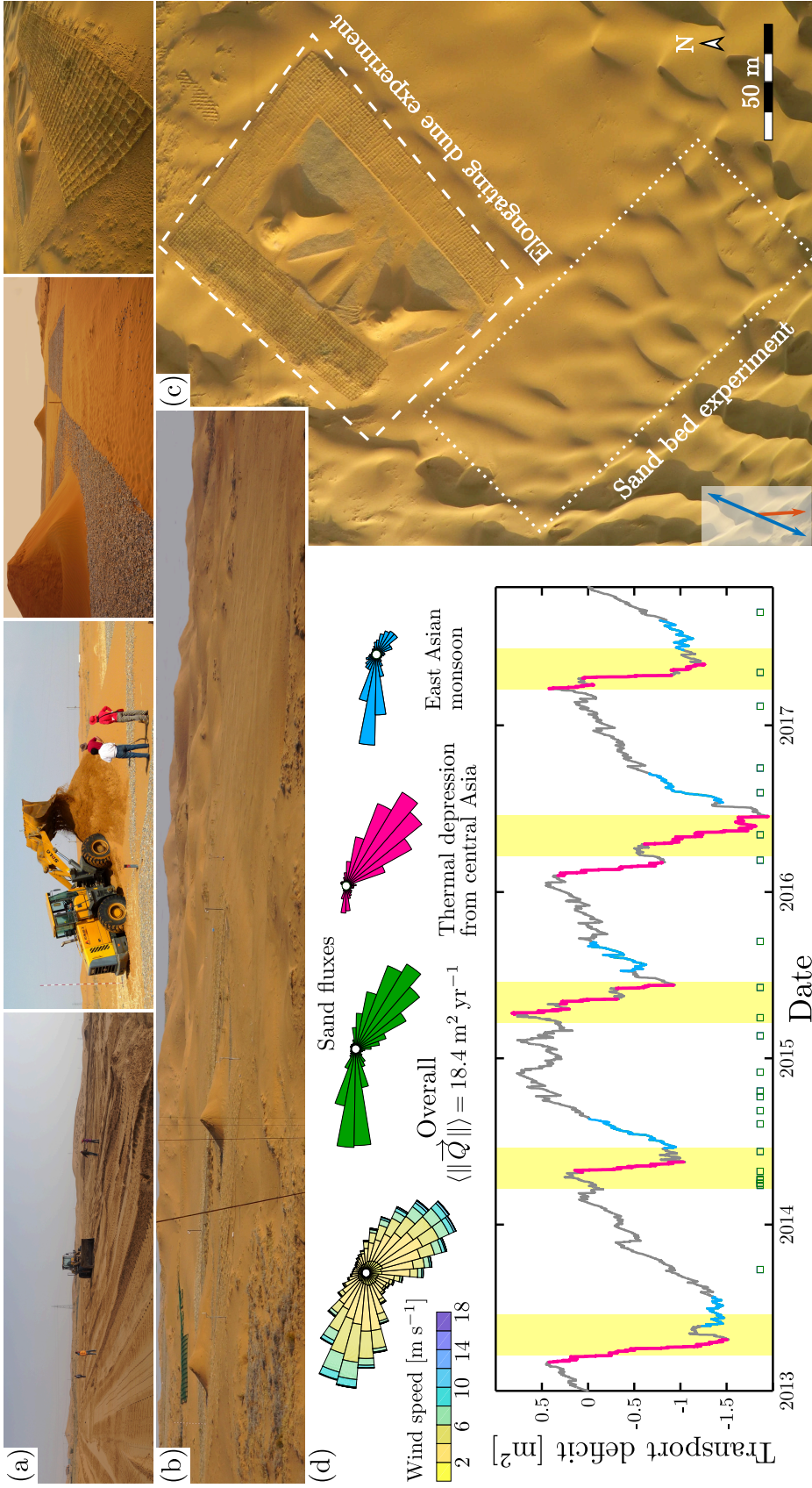


**Figure 1. Landscape-scale experiments on dune growth in the Tengger desert.** (a) Elongating dune experiment in October 2013 (37.560° N, 105.033° E). After leveling (left), sand heaps are placed on a gravel bed (middle) surrounded by straw checkerboards (right). (b) Flat sand bed (on the right) and the elongating dune (on the left) experiments in April 2014. (c) Aerial view of the experimental site in April 2015. Arrows show dune orientations in the bed instability (blue) and the elongating modes (red) predicted from wind data. (d) Wind and sand flux roses from January 2013 to November 2017 and the corresponding variations in transport deficit (Fig. S4 and Supporting Text 3). Specific periods during which primary and secondary winds are highlighted in red and blue, respectively (see the corresponding flux roses). Yellow periods show springs. Squares indicate the dates of topographic surveys.

periment to ensure that the downstream flow field does not affect dune dynamics in the zone of unlimited sediment supply, especially when the easterly wind blows. Thus, the entire experimental setup was designed to promote dune elongation on the gravel bed as well as dune growth and migration on the flat sand bed (arrows in Fig. 1c).

In this area of the Tengger desert, Lü et al. (2021) measured a mean grain size of  $190\ \mu\text{m}$  (Fig. S1, Supporting Text 1) and a threshold shear velocity of  $0.23\pm 0.04\ \text{m s}^{-1}$  for aerodynamic entrainment of sand grains. We use wind data from local meteorological towers and an airport located 10 km east from the experimental dune field (Figs. S2 and S3, Supporting Text 2). We calculate the saturated sand flux on a flat sand bed and at the dune crests using the eolian transport law of Ungar and Haff (1987) (see also Durán et al., 2011) and the formalism of Courrech du Pont et al. (2014) (Tab. S1, Supporting Text 3). Using a reference system of concrete posts, more than 20 ground-based laser scans were performed to frequently measure the evolution of surface elevation in the sand bed and the elongating dune experiments over 4 years (see satellite images in Fig. S5). Point density varied from 470 to 2,370 points per  $\text{m}^2$  with a centimeter height accuracy.

### **From Initial Dune Growth to Long-Term Dynamics**

The two initial sand heaps of the elongating dune experiment were not large enough ( $33$  and  $57\ \text{m}^3$ ) for dune instability or elongation to occur, and they rapidly took a dome dune shape under the effect of the first wind reversals (Bristow & Lancaster, 2004; Gao et al., 2018). Then, seasonal winds lead to complete reworking of the dunes, resulting in successive reorientations of crescentic barchans until April 2015 (Fig. 2a). To allow for dunes to increase their size, we added sand 10 times from May 2013 to September 2016, always in the same places, to rebuild the original sand heaps (Fig. S6, Supporting Text 4). This regular supply is combined with incoming sand fluxes and exchanges of sediments between the two piles, which then evolved into barchan dunes. These mass exchanges benefited to the dune to the southwest, which became larger than the one to the northeast. As both dunes increased in size, their orientation stabilized, adopting an asymmetric barchan shape with a southeast-facing slip face and a longer southern arm.

In the sand bed experiment, the linear phase of the dune instability under unlimited sediment supply was observed from the earliest stage of dune growth, when the residual topography left by the leveling process was smoothed and then disturbed by aeolian

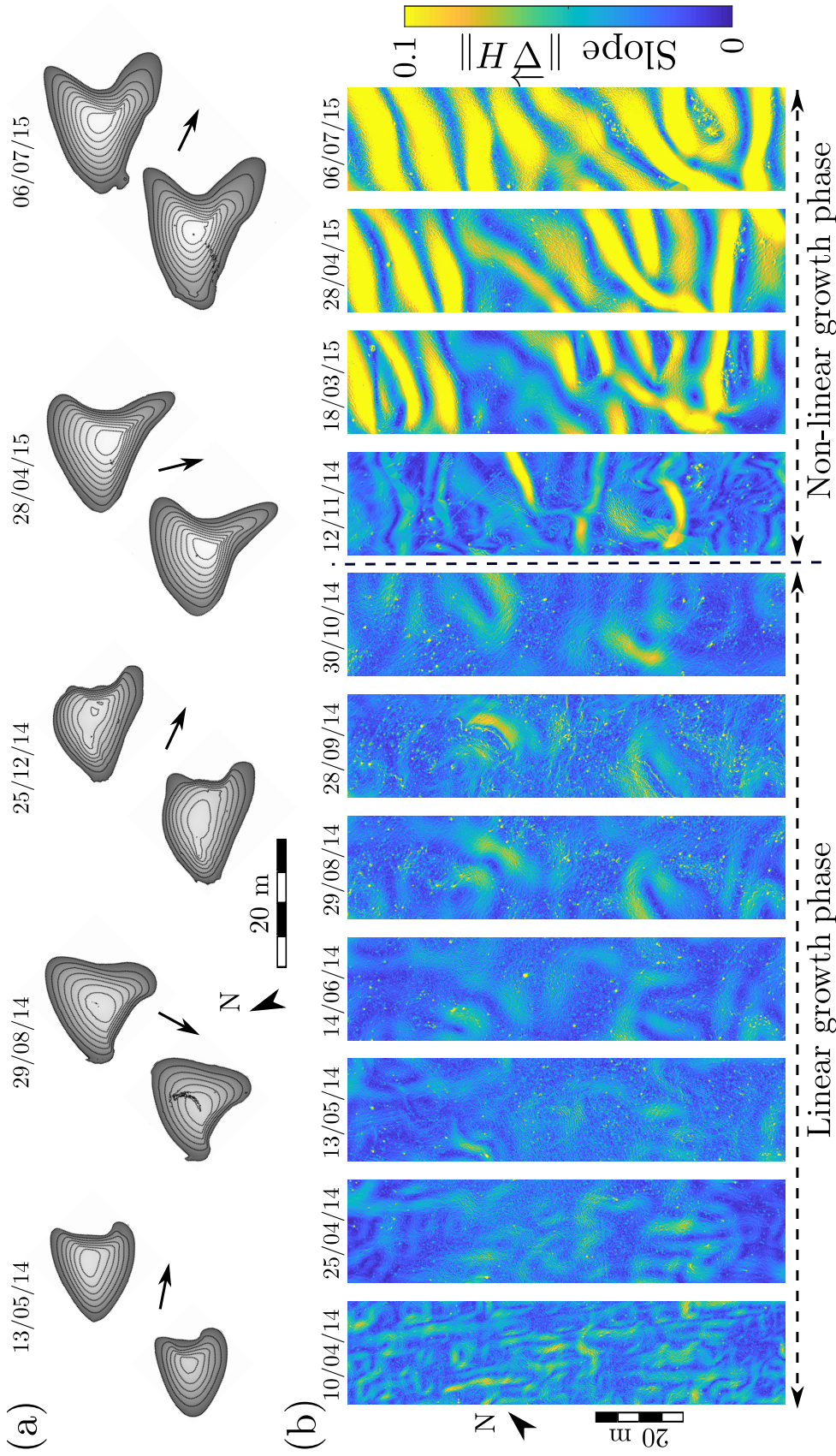


**Figure 2. The early stages of dune growth from April 2014 to July 2015. (a)** Evolution of the two sand heaps of the elongating dune experiments, from dome to barchan and asymmetric barchan shapes. The difference in height between consecutive contours is 25 cm. The lowest contour corresponds to the elevation of the nonerodible bed. Arrows indicate the resultant sand flux direction over the different time intervals. **(b)** Slope maps during incipient dune growth in the sand bed experiment. The colormap is saturated to highlight the transition from the linear to the non-linear phases of the bed instability. In non-saturated areas, ripples can be observed.

transport. During this initial phase, Lü et al. (2021) quantified how growth rate varies with dune wavelength and showed that the highest growth rate was associated with an intermediate length scale of approximately 15 m. This most unstable mode (wavelength) eventually emerged and prevailed across the entire experimental field in November 2014 for mean slope values of 0.07 ( $\approx 4^\circ$ , for both lee and stoss slopes), when the amplitude of topography was less than 20 cm (Fig. 2b). The emergence of this periodic dune pattern reveals the predominance of a southwest-northeast bedform alignment. Then, dunes continued migrating but started growing both in amplitude and wavelength as the non-linear phase of the dune instability took over.

From October 2015 to November 2017, dune pattern coarsening in the sand bed experiment and elongation of the largest asymmetric barchan in the isolated heaps experiment both occurred simultaneously. (Figs. 3a, S7 and S8). In the sand bed experiment, dunes reached a height of 2 m and migrated at an average speed of  $5 \text{ m yr}^{-1}$  from June 2016 to June 2017 (Fig. 3b). They formed a periodic pattern of oblique linear dunes at a  $34^\circ$  angle to the resultant sand flux on a flat sand bed (Hunter et al., 1983; Ping et al., 2014). In the elongating dune experiment, a longitudinal dune developed at an angle of less than 10 degrees to the resulting sand flux. Its total length increased by more than 10 m from April 2016 to June 2017, with a height profile which decreased almost linearly from the sand source area to the tip (Fig. 3c). These observations represent a direct validation in the field of the elongation stages numerically evidenced by Rozier et al. (2019).

## Quantification of Dune Morphodynamics

Frequent acquisition of topographic data allowed for a unique analysis of the two independent growth mechanisms that occur simultaneously. Fig. 4a illustrates the coarsening dynamics of periodic dune patterns and shows that the number of terminations (i.e, defect density) decreased as the characteristic wavelengths of crests and troughs increase (Day & Kocurek, 2018). From April 2015 to November 2017, the wavelength increased from 15 to 25 meters, while the average height  $\langle h \rangle$  tripled from 0.5 to 1.5 meters. These variations lead to a continuous increase in dune aspect ratio (height/wavelength) and an exponential relaxation towards an equilibrium value (Fig. 4b). This coarsening dynamics was closely related to the southeastern migration of the dune pattern, which was directly measured by cross-correlation between successive elevation maps and pre-



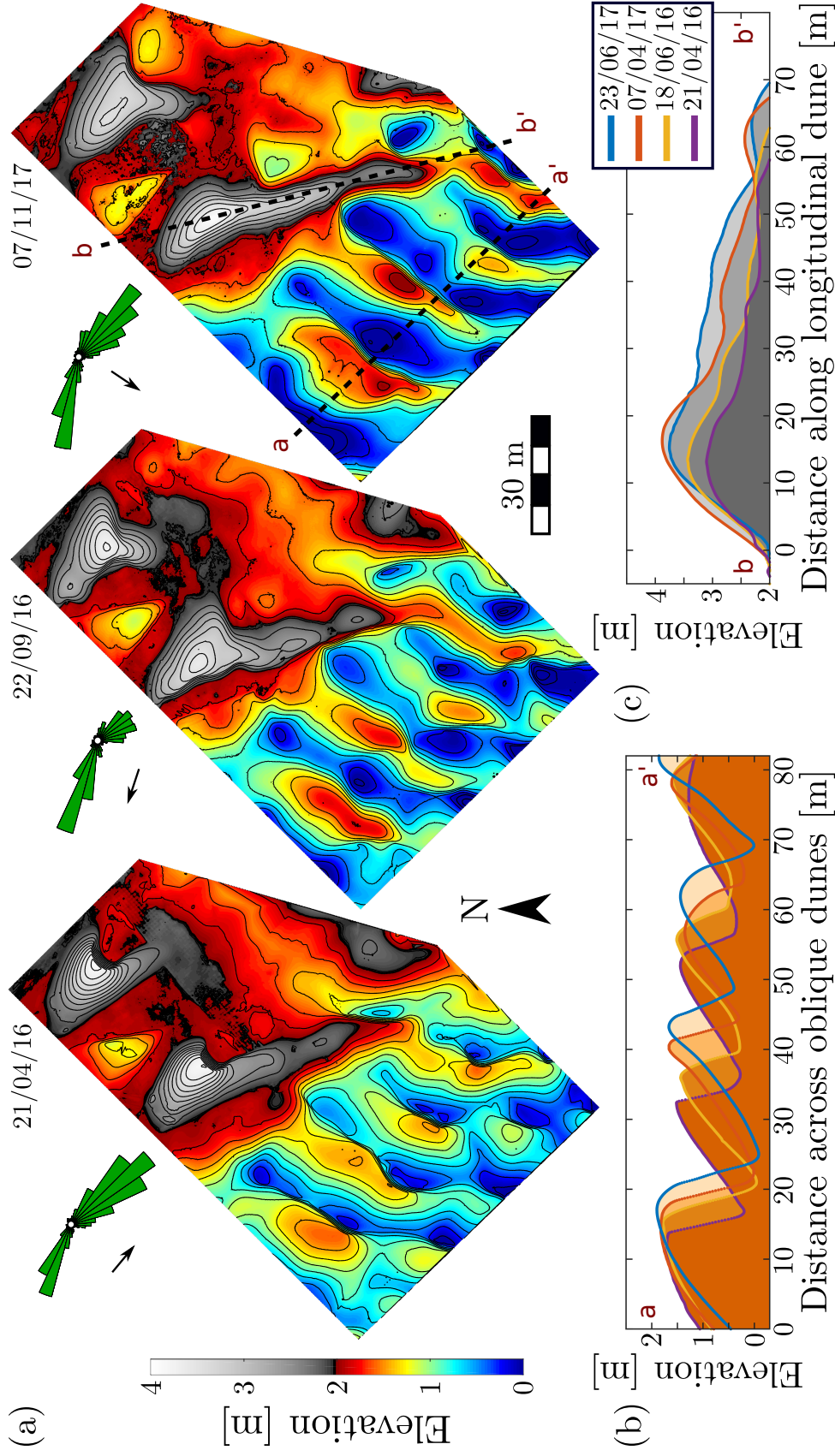


**Figure 3. Coexistence of two dune growth mechanisms starting in April 2016.** (a) Surface elevation of the flat sand bed and the elongating dune experiments. Flux roses show transport directionality over the different time intervals. Arrows indicate the resultant sand flux direction. (b) Migration of oblique linear dunes in the flat sand bed experiment. (c) Elongation of the linear longitudinal dune to the southwest.

dicted from the sand flux at the crest derived from wind data (Fig. 4c). As shown in Fig. 4d, dune orientations of both the elongating dune and in the sand bed experiments were successively compared to the model predictions of Courrech du Pont et al. (2014). The agreement between data-driven predictions and observed orientations and dynamics validates the theoretical approach beyond the initial phase of the dune instability (Lü et al., 2021), under natural wind conditions and for interacting mature bedforms.

Using the elevation of the gravel bed as a reference level for the entire duration of the experiments, we measure the dimensions and volume of the elongating dune as a function of time. Owing to episodic sand input (Fig. S6), the volume of the dune doubled from April 2014 to April 2015, while keeping the aspect ratio between length and width constant (Fig. 4e). Then, a critical volume of  $150 \text{ m}^3$  was reached above which the width of the dune stabilized as the southern arm elongated by more than 10 m in less than a year (Fig. 4f). The positive correlation between the volume and the length-to-width ratio of the dune continued through the end of 2017. Throughout this process, the dune tip maintained a constant size with a transverse width of approximately 5 m and the asymmetric barchan shape can be considered as a transient state in a continuous transition from a barchan to an isolated linear dune shape.

## Discussion

In our landscape-scale experiments, we observed the development of different types of dunes depending on sand availability, and quantified their orientation, dynamics (growth, migration or elongation) and the corresponding sand fluxes at their crests. As shown in Fig. 4, these results not only directly support the model predictions of Courrech du Pont et al. (2014), they also allow to document the early phases of aeolian dune growth with an unprecedented resolution.

Lü et al. (2021) characterized the initial linear phase of the emergence of periodic dunes under unlimited sediment supply from April to December 2014; here, we further characterized the non-linear phase of pattern coarsening over more than 2 years. After the wavelength roughly doubled, the dune aspect-ratio rapidly relaxes toward an equilibrium value, which is similar to that of the surrounding mature dunes in the Tengger Desert (Wen & Dong, 2016). Given the small dune size and their continuous growth, these observations suggest that the dune aspect-ratio is mainly governed by the wind regime,

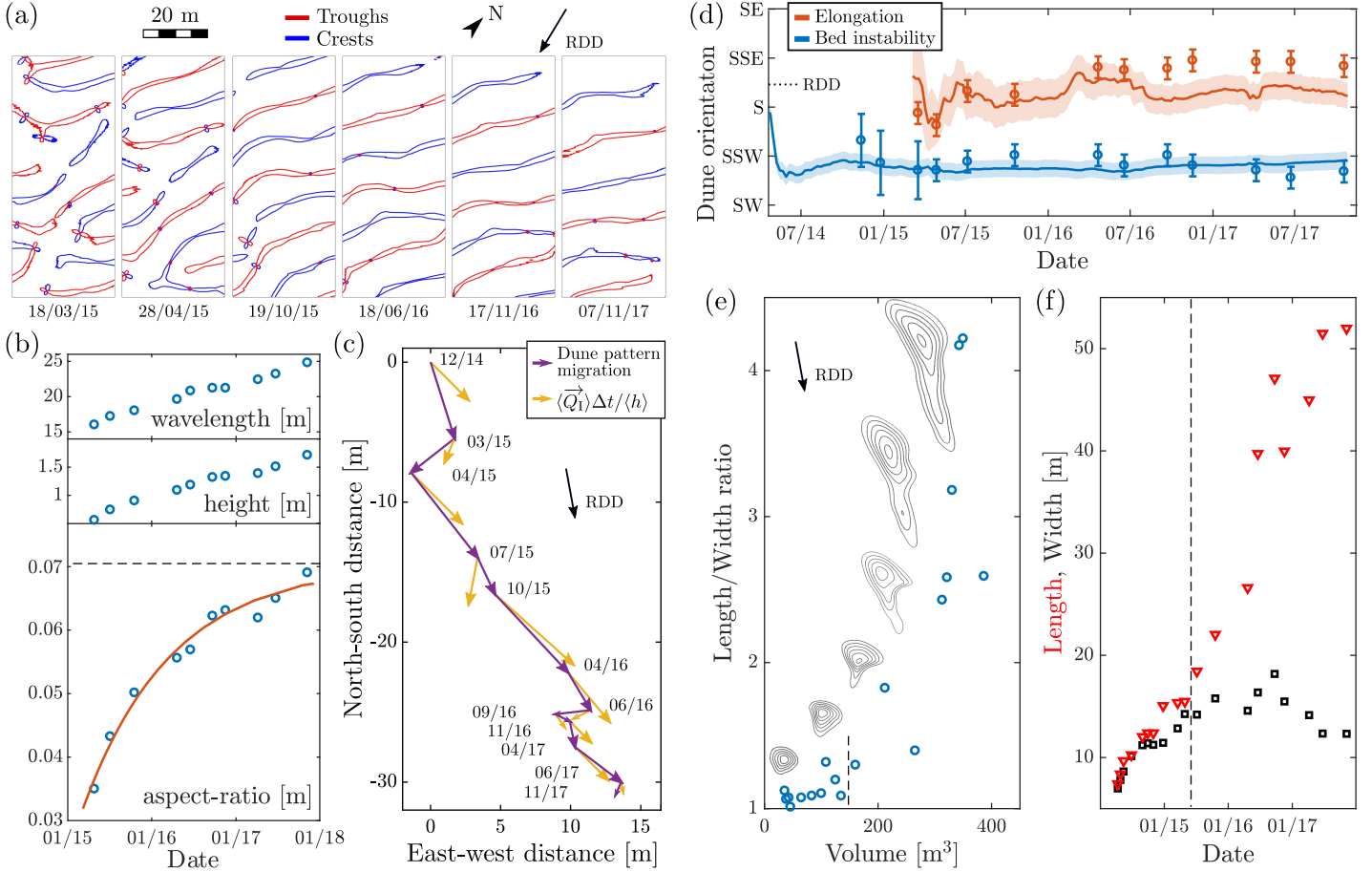


**Figure 4. Dune morphodynamics.** (a) Crests and troughs during dune pattern coarsening in the sand bed experiment. Contours show isolines of  $\text{div}(\nabla h / \|\nabla h\|)$ . Defects produce quadrupole-like structures. The black arrow shows the resultant sand flux direction (RDD). (b) Wavelength, mean amplitude, and aspect ratio of periodic dunes in the sand bed experiment. The red line shows an exponential relaxation towards a plateau value of 0.07 (i.e., a mean slope of 0.14 from troughs to crests). (c) Dune pattern migration obtained by cross-correlation between consecutive elevation maps in the sand bed experiment. The predicted sand flux vectors  $\langle \vec{Q}_i \rangle \Delta t / \langle h \rangle$  at the crest of these periodic dunes are computed from wind data over the corresponding time interval (Tab. S1 and Supporting Text 3). (d) Orientations in the elongating (red) and sand bed (blue) experiments measured from elevation maps by autocorrelation (dots) and predicted from wind data over the cumulative time intervals for grain sizes from 150 to 250  $\mu\text{m}$  and an aerodynamic roughness of  $10^{-4}$  to  $10^{-2}$  m (shaded areas). Errorbars show standard deviations using different radii to integrate the angular energy distribution in autocorrelograms. (e) Length to width ratio of sand heaps in the elongating dune experiment with respect to their volumes. Dunes are shown at different times using contour lines. (f) Sand heaps length and width with respect to time estimated from the distribution of mass above the elevation of the nonerodible bed (Supporting Text 4). Dashed lines show the onset of elongation.

including frequent wind reversals and changes in wind speed, and not by a dune height saturation mechanism. Instead, these changes in dune aspect-ratio certainly contributes to the final dune height by modifying the flow properties over the dunes, especially the upwind shift between the wind speed and the bed topography (Claudin et al., 2013). We also show that the overall migration of the dune pattern during the coarsening phase can be predicted with reasonable accuracy using the normal-to-crest component of transport, with the exception of time periods dominated by the secondary wind. Indeed, crest reversals are not taken into account by the model; adding the strong increase in wind speed-up after wind reversals could improve predictions (Gao et al., 2021).

On a nonerodible bed, we experimentally validated the model for dune elongation and, in the process, showed how larger and larger sand heaps successively produce dome, barchan, and asymmetric barchan shapes (Baddock et al., 2018). A minimum dune volume of  $150 \text{ m}^3$  is required to integrate the local wind variability and initiate elongation. While such threshold behavior has been numerically predicted by Rozier et al. (2019, Fig. 1f), this is the first experimental evidence in the field of a causal relationship between dune shape and size in multidirectional wind regimes. Supporting another prediction of Rozier et al. (2019), we verify that the minimum dune width at the tip is set by  $\lambda_0 \sin(\theta_1)$ , where  $\lambda_0 = 9 \text{ m}$  is the lower cutoff wavelength of the dune instability measured over the same time period in the sand bed experiment (Lü et al., 2021), and  $\theta_1 = 38^\circ$  is the angle between the primary wind and the dune crestline. The stability of the elongating dune relies on the balance between input and output fluxes occurring over the entire length of the dune according to wind strength and orientation. As we regularly fed the original sand-heap and given the limited size of the nonerodible bed, it is difficult to evaluate if a steady length was reached (Rozier et al., 2019). However, considering the resultant sand flux along the crest  $\langle \|\vec{Q}_F\| \rangle = 11.1 \text{ m}^2 \text{ yr}^{-1}$ , as derived from wind data (Tab. S1, Supporting Text 3), we can compute the elongation rate,  $e = \langle \|\vec{Q}_F\| \rangle / h_f$ , where  $h_f$  is dune height at the dune front where width and height decrease rapidly. For a dune front of meter-scale height, this estimate agrees with the elongation rate of  $e \approx 10 \text{ m yr}^{-1}$  observed from April 2016 to June 2017 (see Fig. 3c).

Our landscape-scale experiments conducted in an active dune field provide a quantitative characterization of dune morphogenesis under the natural action of wind for different conditions of sand availability. The elongation of a longitudinal linear dune from a fixed source of sand placed on a nonerodible bed is synchronous with the emergence

and the coarsening of periodic oblique dunes in an area of unlimited sediment supply. This demonstrates that two independent dune growth mechanisms coexist and regulate dune shape, orientation and dynamics according to the boundary conditions and the nature of the bed (i.e., an erodible sand bed or a nonerodible ground). Based on the experimental design and observed bedforms, we show that all these dune properties can be predicted from wind data with increasing accuracy by models that simulate not only the initial growth of dunes (Gadal, Narteau, Ewing, et al., 2020; Lü et al., 2021) but also their morphodynamic response to specific wind cycles (Courrech du Pont et al., 2014; Gao et al., 2018, 2021).

The coexistence of two growth mechanisms naturally explains some of the natural complexities of dune fields, and offer new perspectives to Earth-based and planetary geologists studying the evolution of sand seas of the solar system. Dunes and superimposed bedforms with different shapes and orientations can now be studied according to elementary dune types relying on two independent dune growth mechanisms. This effort devoted to questions of pattern emergence and organization is critical to predict the evolution of eolian dune systems according to changes in climate and wind properties.

## **Data Availability**

All study data are included in the article and/or SI Appendix. Elevation and wind data are available on <https://doi.org/10.6084/m9.figshare.17817494.v4>.

## **Author contributions**

P.L. and C.N. carried out all statistical data analysis and numerical simulations, helped by C.G.. P.L., C.N., P.C., S.R. and S.C.P. designed the experimental study. P.L., C.N. and Z.D. managed the experimental site and P.L. led the acquisition of data in the field. Z.A. performed all laser scans. C.N., P.C., S.R. and S.C.P. wrote the manuscript. All authors participate to data acquisition and discussed the results.

## **Acknowledgments**

We acknowledge financial support from National Natural Science Foundation of China Grants 41871011 and 41930641, Laboratoire d'Excellence UnivEarthS Grant ANR-10-LABX-0023, Initiative d'Excellence Université de Paris Grant ANR-18-IDEX-0001, French National Research Agency Grants ANR-12-BS05-001-03/EXO-DUNES and ANR-17-CE01-0014/SONO, National Science Center of Poland Grant 2016/23/B/ST10/01700, and the French Chinese International Laboratory on Sediment Transport and Landscape Dynamics.

## References

- Andreotti, B., Claudin, P., & Douady, S. (2002, August). Selection of dune shapes and velocities: Part 2: A two-dimensional modelling. *Eur. Phys. J. B*, *28*(3), 341-352.
- Baddock, M. C., Nield, J. M., & Wiggs, G. F. (2018). Early-stage aeolian protodunes: Bedform development and sand transport dynamics. *Earth Surface Processes and Landforms*, *43*(1), 339–346.
- Bagnold, R. A. (1941). *The physics of wind blown sand and desert dunes* (Vol. 265). Methuen, London.
- Bristow, C., & Lancaster, N. (2004). Movement of a small slipfaceless dome dune in the Namib Sand Sea, Namibia. *Geomorphology*, *59*(1), 189 - 196. doi: <https://doi.org/10.1016/j.geomorph.2003.09.015>
- Chanteloube, C., Barrier, L., Derakhshani, R., Gadal, C., Braucher, R., Payet, V., ... Narteau, C. (2022). Source-to-sink aeolian fluxes from arid landscape dynamics in the lut desert. *Geophysical Research Letters*, e2021GL097342.
- Claudin, P., Wiggs, G., & Andreotti, B. (2013). Field evidence for the upwind velocity shift at the crest of low dunes. *Boundary-layer meteorology*, *148*(1), 195–206.
- Courrech du Pont, S., Narteau, C., & Gao, X. (2014). Two modes for dune orientation. *Geology*, *42*(9), 743–746. doi: 10.1130/G35657.1
- Day, M., & Kocurek, G. (2018). Pattern similarity across planetary dune fields. *Geology*, *46*(11), 999–1002.
- Delorme, P., Wiggs, G. F., Baddock, M. C., Claudin, P., Nield, J. M., & Valdez, A. (2020). Dune initiation in a bimodal wind regime. *Journal of Geophysical Research: Earth Surface*, *125*(11), e2020JF005757.
- Durán, O., Claudin, P., & Andreotti, B. (2011). On aeolian transport: Grain-scale interactions, dynamical mechanisms and scaling laws. *Aeolian Research*, *3*(3), 243–270.
- Ewing, R. C., & Kocurek, G. A. (2010). Aeolian dune interactions and dune-field pattern formation: White Sands Dune Field, New Mexico. *Sedimentology*, *57*(5), 1199–1219.
- Ewing, R. C., Peyret, A.-P. B., Kocurek, G., & Bourke, M. (2010). Dune field pattern formation and recent transporting winds in the Olympia Undae dune

- field, north polar region of Mars. *Journal of Geophysical Research: Planets*, *115*(E8).
- Fenton, L. K., & Hayward, R. K. (2010). Southern high latitude dune fields on Mars: Morphology, aeolian inactivity, and climate change. *Geomorphology*, *121*(1-2), 98–121.
- Fernandez-Cascales, L., Lucas, A., Rodriguez, S., Gao, X., Spiga, A., & Narteau, C. (2018). First quantification of relationship between dune orientation and sediment availability, Olympia Undae, Mars. *Earth and Planetary Science Letters*, *489*, 241–250.
- Gadal, C., Narteau, C., Courrech du Pont, S., Rozier, O., & Claudin, P. (2020). Periodicity in fields of elongating dunes. *Geology*, *48*, 343–347.
- Gadal, C., Narteau, C., du Pont, S. C., Rozier, O., & Claudin, P. (2019). Incipient bedforms in a bidirectional wind regime. *Journal of Fluid Mechanics*, *862*, 490–516.
- Gadal, C., Narteau, C., Ewing, R. C., Gunn, A., Jerolmack, D., Andreotti, B., & Claudin, P. (2020). Spatial and temporal development of incipient dunes. *Geophysical Research Letters*, *47*(16), e2020GL088919.
- Gao, X., Gadal, C., Rozier, O., & Narteau, C. (2018). Morphodynamics of barchan and dome dunes under variable wind regimes. *Geology*, *46*(9), 743. doi: 10.1130/G45101.1
- Gao, X., Narteau, C., & Gadal, C. (2021). Migration of reversing dunes against the sand flow path as a singular expression of the speed-up effect. *Journal of Geophysical Research: Earth Surface*, *126*(5), e2020JF005913. doi: <https://doi.org/10.1029/2020JF005913>
- Gao, X., Narteau, C., & Rozier, O. (2015). Development and steady states of transverse dunes: A numerical analysis of dune pattern coarsening and giant dunes. *J. Geophys. Res.*, *120*, 2200–2219.
- Gao, X., Narteau, C., Rozier, O., & Courrech du Pont, S. (2015). Phase diagrams of dune shape and orientation depending on sand availability. *Scientific reports*, *5*, 14677. doi: 10.1038/srep14677
- Hunter, R. E., Richmond, B. M., et al. (1983). Storm-controlled oblique dunes of the oregon coast. *Geol. Soc. Am. Bull.*, *94*(12), 1450–1465.
- Jarvis, P., Bacik, K., Narteau, C., & Vriend, N. (2022). Coarsening dynamics



- of 2D subaqueous dunes. *Journal of Geophysical Research: Earth Surface*, e2021JF006492.
- Kennedy, J. (1963). The mechanics of dunes and antidunes in erodible bed channels. *J. Fluid Mech.*, 16, 521–544.
- Kocurek, G., & Ewing, R. (2005). Aeolian dune field self-organization—implications for the formation of simple versus complex dune-field patterns. *Geomorphology*, 72(1), 94–105.
- Lapôtre, M., Ewing, R., Lamb, M., Fischer, W., Grotzinger, J., Rubin, D., . . . others (2016). Large wind ripples on Mars: A record of atmospheric evolution. *Science*, 353(6294), 55–58.
- Lapôtre, M., Ewing, R., Weitz, C., Lewis, K., Lamb, M., Ehlmann, B., & Rubin, D. (2018). Morphologic diversity of martian ripples: Implications for large-ripple formation. *Geophysical Research Letters*, 45(19), 10–229.
- Lapôtre, M. G., Ewing, R. C., & Lamb, M. P. (2021). An evolving understanding of enigmatic large ripples on mars. *Journal of Geophysical Research: Planets*, 126(2), e2020JE006729.
- Lorenz, R. D., & Zimelman, J. R. (2014). *Dune worlds*. Springer.
- Lü, P., Narteau, C., Dong, Z., Claudin, P., Rodriguez, S., An, Z., . . . Courrech du Pont, S. (2021). Direct validation of dune instability theory. *Proceedings of the National Academy of Sciences*, 118(17).
- Lü, P., Narteau, C., Dong, Z., Rozier, O., & Courrech Du Pont, S. (2017). Unravelling raked linear dunes to explain the coexistence of bedforms in complex dunefields. *Nature Communications*, 8, 14239.
- Lucas, A., Narteau, C., Rodriguez, S., Rozier, O., Callot, Y., Garcia, A., & Courrech du Pont, S. (2015). Sediment flux from the morphodynamics of elongating linear dunes. *Geology*, 43(11), 1027–1030.
- Lucas, A., Rodriguez, S., Narteau, C., Charnay, B., Pont, S. C., Tokano, T., . . . others (2014). Growth mechanisms and dune orientation on Titan. *Geophysical Research Letters*, 41(17), 6093–6100.
- Parteli, E., Durán, O., Tsoar, H., Schwämmle, V., & Herrmann, H. (2009). Dune formation under bimodal winds. *Proc. Natl. Acad. Sci. USA*, 1106(52), 22085–22089. doi: 10.1073/pnas.0808646106
- Ping, L., Narteau, C., Dong, Z., Zhang, Z., & Courrech du Pont, S. (2014). Emer-

- gence of oblique dunes in a landscape-scale experiment. *Nature Geoscience*, *7*, 99–103. doi: 10.1038/ngeo2047
- Reffet, E., Courrech du Pont, S., Hersen, P., & Douady, S. (2010). Formation and stability of transverse and longitudinal sand dunes. *Geology*, *38*(6), 491–494.
- Richards, K. J. (1980). The formation of ripples and dunes on an erodible bed. *J. Fluid Mech.*, *99*(03), 597–618.
- Rozier, O., Narteau, C., Gadal, C., Claudin, P., & Courrech du Pont, S. (2019). Elongation and stability of a linear dune. *Geophysical Research Letters*, *46*, 14521–14530.
- Rubin, D., & Hunter, R. (1987). Bedform alignment in directionally varying flows. *Science*, *237*, 276–278.
- Telfer, M. W., Parteli, E. J., Radebaugh, J., Beyer, R. A., Bertrand, T., Forget, F., ... others (2018). Dunes on pluto. *Science*, *360*(6392), 992–997.
- Ungar, J., & Haff, P. (1987). Steady state saltation in air. *Sedimentology*, *34*(2), 289–299.
- Wasson, R., & Hyde, R. (1983). Factors determining desert dune types. *Nature*, *304*, 337–339.
- Wen, Q., & Dong, Z. (2016). Geomorphologic patterns of dune networks in the tengger desert, china. *Journal of Arid Land*, *8*(5), 660–669.
- Zhang, D., Narteau, C., Rozier, O., & Courrech du Pont, S. (2012). Morphology and dynamics of star dunes from numerical modelling. *Nature Geoscience*, *5*(7), 463–467.

## References From the Supporting Information

- Courrech du Pont, S., Narteau, C., & Gao, X. (2014). Two modes for dune orientation. *Geology*, *42*(9), 743–746. doi: 10.1130/G35657.1
- Dempster, A. P., Laird, N. M., & Rubin, D. B. (1977). Maximum likelihood from incomplete data via the em algorithm. *Journal of the Royal Statistical Society: Series B (Methodological)*, *39*(1), 1–22.
- Durán, O., Claudin, P., & Andreotti, B. (2011). On aeolian transport: Grain-scale interactions, dynamical mechanisms and scaling laws. *Aeolian Research*, *3*(3), 243–270.
- Elbelrhiti, H., Andreotti, B., & Claudin, P. (2008). Barchan dune corridors: field

- characterization and investigation of control parameters. *J. Geophys. Res.*, *113*(F02S15).
- Field, J., & Pelletier, J. (2018). Controls on the aerodynamic roughness length and the grain-size dependence of aeolian sediment transport. *Earth Surface Processes and Landforms*, *43*, 2616–2626.
- Fryberger, S. G., & Dean, G. (1979). Dune forms and wind regime. *A study of global sand seas, 1052*, 137–169.
- Gadal, C., Narteau, C., du Pont, S. C., Rozier, O., & Claudin, P. (2019). Incipient bedforms in a bidirectional wind regime. *Journal of Fluid Mechanics*, *862*, 490–516.
- Gao, X., Narteau, C., Rozier, O., & Courrech du Pont, S. (2015). Phase diagrams of dune shape and orientation depending on sand availability. *Scientific reports*, *5*, 14677. doi: 10.1038/srep14677
- Hersen, P. (2004, February). On the crescentic shape of barchan dunes. *European Physical Journal B*, *37*(4), 507-514.
- Hunter, R. E., Richmond, B. M., et al. (1983). Storm-controlled oblique dunes of the oregon coast. *Geological Society of America Bulletin*, *94*(12), 1450–1465.
- Iversen, J. D., & Rasmussen, K. R. (1999). The effect of wind speed and bed slope on sand transport. *Sedimentology*, *46*(4), 723–731.
- Jackson, P. S., & Hunt, J. C. R. (1975). Turbulent wind flow over a low hill. *Q. J. R. Meteorol. Soc.*, *101*, 929.
- Lü, P., Narteau, C., Dong, Z., Claudin, P., Rodriguez, S., An, Z., . . . Courrech du Pont, S. (2021). Direct validation of dune instability theory. *Proceedings of the National Academy of Sciences*, *118*(17). doi: 10.1073/pnas.2024105118
- Lü, P., Narteau, C., Dong, Z., Rozier, O., & Courrech Du Pont, S. (2017). Unravelling raked linear dunes to explain the coexistence of bedforms in complex dunefields. *Nature Communications*, *8*, 14239.
- Lucas, A., Narteau, C., Rodriguez, S., Rozier, O., Callot, Y., Garcia, A., & Courrech du Pont, S. (2015). Sediment flux from the morphodynamics of elongating linear dunes. *Geology*, *43*(11), 1027–1030.
- Owen, P. R. (1964). Saltation of uniformed sand grains in air. *J. Fluid. Mech.*, *20*, 225–242.
- Pearce, K. I., & Walker, I. J. (2005). Frequency and magnitude biases in the ‘Fry-

- berger' model, with implications for characterizing geomorphically effective winds. *Geomorphology*, *68*(1), 39–55.
- Ping, L., Narteau, C., Dong, Z., Zhang, Z., & Courrech du Pont, S. (2014). Emergence of oblique dunes in a landscape-scale experiment. *Nature Geoscience*, *7*, 99–103. doi: 10.1038/ngeo2047
- Rozier, O., Narteau, C., Gadal, C., Claudin, P., & Courrech du Pont, S. (2019). Elongation and stability of a linear dune. *Geophysical Research Letters*, *46*, 14521–14530. doi: 10.1029/2019GL085147
- Rubin, D., & Hunter, R. (1987). Bedform alignment in directionally varying flows. *Science*, *237*, 276–278.
- Sherman, D. J., & Farrell, E. J. (2008). Aerodynamic roughness lengths over movable beds: Comparison of wind tunnel and field data. *Journal of Geophysical Research: Earth Surface*, *113*(F02S08).
- Tsoar, H. (2005). Sand dunes mobility and stability in relation to climate. *Physica A*, *357*(1), 50–56.
- Ungar, J., & Haff, P. (1987). Steady state saltation in air. *Sedimentology*, *34*(2), 289–299.
- Zhang, D., Yang, X., Rozier, O., & Narteau, C. (2014). Mean sediment residence time in barchan dunes. *J. Geophys. Res.*, *119*, 451–463. doi: 10.1002/2013JF002833